

SPECT of Transplanted Islets of Langerhans by Dopamine 2 Receptor Targeting in a Rat Model

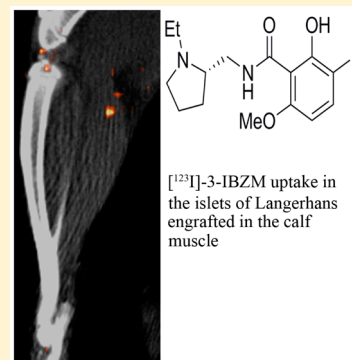
Stefanie M. A. Willekens,^{*,†} Inge van der Kroon,[†] Lieke Joosten,[†] Cathelijne Frielink,[†] Otto C. Boerman,[†] Sebastiaan A. M. W. van den Broek,[‡] Maarten Brom,[†] and Martin Gotthardt[†]

[†]Department of Radiology and Nuclear Medicine, Radboud University Medical Center, PO Box 9101, 6500 HB Nijmegen, The Netherlands

[‡]FutureChemistry Holding BV, Toernooiveld 100, 6525 EC Nijmegen, The Netherlands

ABSTRACT: Pancreatic islet transplantation can be a more permanent treatment for type 1 diabetes compared to daily insulin administration. Quantitative and longitudinal noninvasive imaging of viable transplanted islets might help to further improve this novel therapy. Since islets express dopamine 2 (D2) receptors, they could be visualized by targeting this receptor. Therefore, the D2 receptor antagonist based tracer [¹²⁵I]-3-IBZM was selected to visualize transplanted islets in a rat model. IBZM was radioiodinated, and the labeling was optimized for position 3 of the aromatic ring. [¹²⁵I]-3-IBZM was characterized in vitro using INS-1 cells and isolated islets. Subsequently, 1,000 islets were transplanted in the calf muscle of WAG/Rij rats and SPECT/CT images were acquired 6 weeks after transplantation. Finally, the graft containing muscle was dissected and analyzed immunohistochemically. Oxidative radioiodination resulted in 3 IBZM isomers with different receptor affinities. The use of 0.6 mg/mL chloramine-T hydrate resulted in high yield formation of predominantly [¹²⁵I]-3-IBZM, the isomer harboring the highest receptor affinity. The tracer showed D2 receptor mediated binding to isolated islets in vitro. The transplant could be visualized by SPECT 6 weeks after transplantation. The transplants could be localized in the calf muscle and showed insulin and glucagon expression, indicating targeting of viable and functional islets in the transplant. Radioiodination was optimized to produce high yields of [¹²⁵I]-3-IBZM, the isomer showing optimal D2R binding. Furthermore, [¹²⁵I]-3-IBZM specifically targets the D2 receptors on transplanted islets. In conclusion, this tracer shows potential for noninvasive in vivo detection of islets grafted in the muscle by D2 receptor targeting.

KEYWORDS: iodination, IBZM, SPECT, islets of Langerhans, transplantation



INTRODUCTION

For patients suffering from type 1 diabetes, insulin is never a cure, only a treatment. Pancreatic islet transplantation could be a permanent solution for these patients. Unfortunately, insulin independency drops to less than 15% five years after transplantation.¹ Currently, graft function is monitored by measuring functional biomarkers, such as C-peptide and HbA_{1c} levels, which show large interindividual differences and are delayed markers for islet loss.² Furthermore, it has been shown that beta cell function is not always a representative measure for the remaining beta cell mass.^{3,4} Therefore, visualization of the remaining viable graft volume might provide important information on the metabolic state of the islet graft.⁵ A possible method to accurately monitor islet loss is longitudinal quantitative imaging. Noninvasive imaging modalities like single photon emission computed tomography (SPECT) and positron emission tomography (PET) could provide important insights into the fate of transplanted islets⁶ and could help to improve the outcome of this promising therapeutic approach.

Several attempts have been made to visualize transplanted islets, using different imaging modalities. Transplanted islets, prelabeled with a paramagnetic contrast agent, could be visualized using magnetic resonance imaging (MRI).^{7,8} Besides

MRI, transplanted islets can also be imaged using PET or SPECT. The first results of imaging the graft by PET date from 2006, where islets, transfected with a reporter gene or an adenoviral vector, could be visualized using ¹⁸F-fluorohydroxybutylguanine (¹⁸F-FHBG) as a tracer.^{9,10} Furthermore, ¹⁸F-fluorodeoxyglucose (¹⁸F-FDG) showed potential to image immediate events following transplantation.^{11,12} Transplanted islets were also imaged by SPECT and PET using ¹¹¹In-labeled exendin-4.¹³ In fact exendin appears to be useful for longitudinal graft imaging.¹⁴ Nevertheless, the use of alternative tracers, in addition to exendin, might help to gain important complementary information about the islet graft, such as metabolic stress, inflammatory processes, dedifferentiation, and rejection. In other words, alternative tracers might allow more complete characterization of islet grafts.

One of these potential alternative tracers is iodobenzamide (IBZM, Figure 1), a molecule with strong antidopaminergic activity and very high specificity for the dopamine 2 (D2)

Received: June 30, 2015

Revised: November 20, 2015

Accepted: November 25, 2015

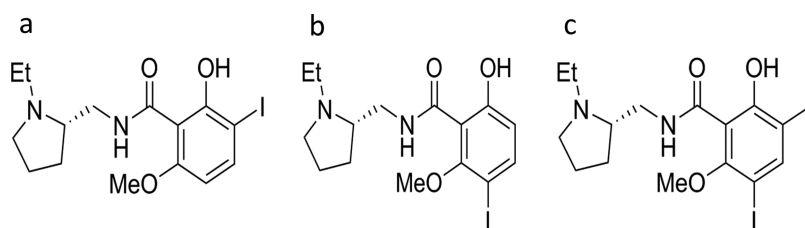


Figure 1. Chemical structures of (a) 3-IBZM, (b) 5-IBZM, and (c) 3,5-di-IBZM.

receptor. Labeled with iodine-123, this molecule is clinically used for D2 receptor imaging in neurodegenerative diseases.^{15,16} Furthermore, D2 receptors are expressed in pancreatic islets, where they mediate insulin secretion upon dopamine binding.^{17,18} Consequently, [¹²³I]IBZM may be a promising candidate to target transplanted islets via the D2 receptor.

In this study, we determined the potential of iodinated benzamide (BZM) for imaging of transplanted islets of Langerhans. The radioiodination of BZM was optimized for iodination of the 3 position of the aromatic ring, since different substitutions on this ring resulted in molecules with different affinity for the receptor. The *in vitro* binding properties of the tracer were characterized, and finally, islets engrafted in the calf muscle of WAG/Rij rats were visualized by SPECT after injection of [¹²³I]IBZM.

MATERIALS AND METHODS

Compounds and Radionuclides. BZM and IBZM were purchased from ABX (advanced biochemical compounds, Radeberg, Germany). [¹²³I]IBZM and sodium [¹²⁵I]iodide were obtained from GE healthcare (Eindhoven, Netherlands) and PerkinElmer (Boston, MA, USA), respectively.

Radiolabeling. BZM was iodinated using oxidative iodination, as described previously.¹⁵ The effect of the chloramine-T concentration on the reaction product was determined. Briefly, chloramine-T hydrate (15 μ L; 0.6, 0.9, or 1.2 mg/mL) was added to a mixture of BZM (25 μ L, 10 mg/mL), 10 μ L of 0.5 M phosphate buffer, and 5 MBq of Na[¹²⁵I]. After incubation for 2 min at room temperature, the reaction was quenched using 200 μ L of metabisulfite (1 mg/mL). Reaction products were purified by reversed-phase high performance liquid chromatography (RP-HPLC) using an Eclipse XDB C18 column (Agilent Technologies, Santa Clara, CA, USA). The column was eluted with 0.1% trifluoroacetic acid (TFA) in H₂O (0–5 min) followed by a linear gradient from 3% to 100% acetonitrile with 0.1% TFA over 30 min (flow rate: 1 mL/min). The fractions containing [¹²⁵I]IBZM were collected and diluted with RPMI 1640 medium (Invitrogen, Camarillo, CA, USA) containing 0.5% (w/v) bovine serum albumin (BSA).

Cell Culture. The rat insulinoma cell line INS-1 was cultured as described previously.¹⁹ In short, cells were maintained in RPMI supplemented with 10% fetal bovine serum (FCS) (HyClone, Celbio, Logan, UT, USA), 2 mM L-glutamine (Sigma-Aldrich, St. Louis, MO, USA), 10 mM HEPES (Invitrogen), 50 μ M β -mercaptoethanol (ICN Biomedicals Inc., Aurora, OH, USA), 1 mM sodium pyruvate (Invitrogen), 100 U/mL penicillin (Sigma-Aldrich), and 100 μ g/mL streptomycin (Sigma-Aldrich), in a humidified atmosphere containing 5% CO₂ at 37 $^{\circ}$ C.

In Vitro Binding to INS-1 Cells. INS-1 cells were harvested by trypsinization, transferred to Eppendorf tubes (3×10^6 cells per tube), and washed twice with binding buffer (RPMI containing 0.5% BSA (w/v)). Approximately 1,600 Bq of [¹²⁵I]IBZM (20.5 fmol) was added followed by incubation for 4 h at 37 $^{\circ}$ C. After incubation, cells were washed twice with binding buffer and cell-associated radioactivity was measured in a well type gamma counter (Wallac 1480 wizard, PerkinElmer).

In Vitro Internalization. The internalization kinetics of [¹²⁵I]IBZM were determined as described previously²⁰ using suspensions of INS-1 cells (3×10^6 cells per tube). The cells were resuspended in binding buffer along with approximately 1,600 cpm [¹²⁵I]IBZM (20.5 fmol) and incubated for 1, 2, or 4 h at 37 $^{\circ}$ C. After incubation, the cells were washed twice with binding buffer. To determine the surface-bound radiolabeled fraction, ice-cold acid buffer (0.1 M acetic acid, 154 mM NaCl, pH 2.5) was added and cells were incubated for 10 min at 4 $^{\circ}$ C. After washing the cells twice with binding buffer, the cell-associated activity was measured in a gamma counter. The internalized fraction (cell-associated activity after acid wash) and the receptor-bound fraction (activity removed by acid wash) were determined.

Animals. Female Wistar Albino Glaxo (WAG)/Rij rats, 6–8 weeks old (Charles River Laboratories, Erkrath, Sulzfeld, Germany), were used as islet donors and recipients. Animals were provided with food and water *ad libitum*. Animal experiments were approved by the animal welfare committee of the Radboud University Nijmegen.

Islet Isolation. In order to validate the results obtained using INS-1 cells, D2 receptor binding of the tracer was further analyzed using isolated islets. Pancreatic islets were isolated from WAG/Rij rats by collagenase digestion. Rats were euthanized by CO₂/O₂ suffocation, and 8 mL of ice cold RPMI 1640 containing 1 mg/mL collagenase type V (Sigma-Aldrich) were infused via the pancreatic duct *in situ*. After dissection, the perfused pancreata were collected in serum free medium containing collagenase and kept on ice until digestion. Pancreata were digested for 11 min and 30 s at 37 $^{\circ}$ C. Digestion was stopped by adding RPMI medium containing 10% FCS, 2 mM L-glutamine, 100 U/mL penicillin, and 100 U/mL streptomycin (complete RPMI). After washing, digested pancreata were passed through a mesh. Afterward, islets were purified on a discontinuous Ficoll gradient (densities: 1.108; 1.096; 1.037; Cellgro by Mediatech Inc., Manassas, VA, USA) by centrifugation at 625g for 16 min without brake. Islets were collected from the intersection of the second and third layer and remaining Ficoll was removed by washing with complete RPMI. Isolated islets were cultured overnight in complete RPMI medium in a humidified atmosphere containing 5% CO₂ at 37 $^{\circ}$ C.

In Vitro Binding to Isolated Islets. After overnight recovery, islets were collected, counted, and resuspended in complete RPMI. Islets were divided in 24 well Transwell plates

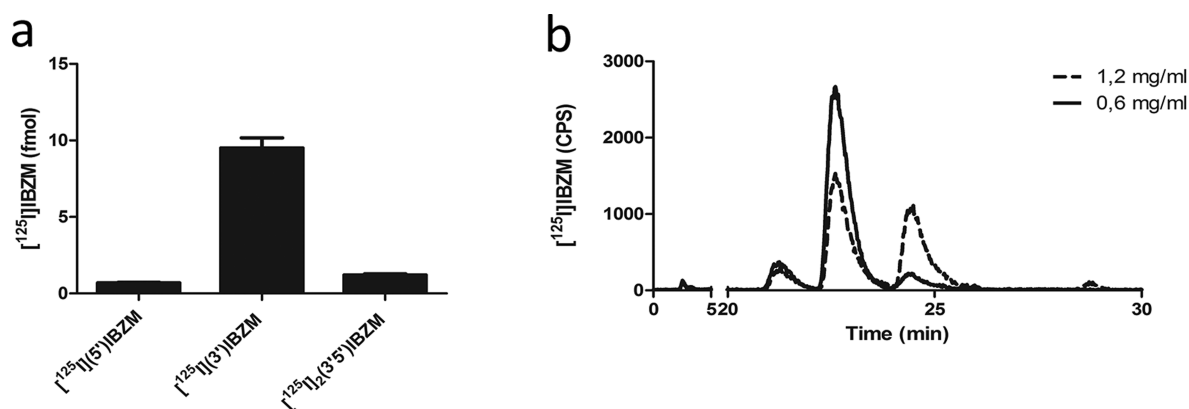


Figure 2. (a) Cell binding of the different IBZM analogues to INS-1 cells. (b) Elution profile of the reaction products at various concentrations of chloramine-T hydrate.

(600 islets per Transwell) (Corning Inc., Tewksbury, MA, USA) and washed with binding buffer. Subsequently, approximately 1,600 cpm of [¹²⁵I]-3-IBZM was added followed by incubation for 4 h at 37 °C. To examine D2 receptor mediated uptake, 5 μg of unlabeled IBZM was added together with [¹²⁵I]-3-IBZM to separate wells. After incubation, islets were washed with binding buffer and islet associated radioactivity was determined in a well type gamma counter.

Islet Transplantation. Isolated islets were collected, resuspended, and counted in RPMI medium without supplements. Healthy recipient rats were anesthetized using isoflurane (induction 4–5%, maintenance 2% in 80% O₂ and 20% N₂O) (Abbott Laboratories, Toronto, Canada), and the right hind leg was shaved and disinfected with Betadine (Meda Pharma B.V., Amstelveen, The Netherlands) prior to islet injection. Thousand islets were aspirated into a catheter line and infused manually at a constant, low speed into the calf muscle using a Hamilton syringe (100 ± 17.3 μL) (Hamilton Company, Reno, NV, USA).

SPECT Acquisition, Reconstruction, and Biodistribution. Six weeks after transplantation, the rats (*n* = 3), transplanted with 1,000 islets, were injected with 53.7 ± 6.1 MBq of [¹²³I]IBZM (IBZM dose 1.7 ng in 500 μL of injection fluid) in the tail vein. One hour after injection, SPECT images were acquired under inhalation (isoflurane) anesthesia on a USPECTII/CT small animal scanner (MILabs, Utrecht, Netherlands) for 50 min using a 1 mm pinhole general purpose rat and mouse collimator. CT was performed as an anatomical reference with the following settings: spatial resolution 160 μm; 65 kV and 615 μA. SPECT scans were reconstructed using the USPECT reconstruction software (MILabs, Utrecht, Netherlands) with the following settings: selection of the ¹²³I photopeak (143–175 keV) corrected for background (175–200 keV), pixel based OSEM, voxel size 0.75 mm, 2 iterations, and 16 subsets. After SPECT/CT acquisition, rats were euthanized by CO₂/O₂ suffocation and the muscle containing the transplant and other relevant tissues (blood, muscle, heart, lung, spleen, pancreas, kidney, liver, stomach, and duodenum) was dissected, weighed, and measured in a well type gamma counter to determine the distribution of the tracer over the different organs. Unfortunately, in vivo competition studies could not be performed due to the lethal effects of such high IBZM dose.

Immunohistochemistry. Graft containing muscles were fixed in 4% formalin, dehydrated, and embedded in paraffin. Sections (4 μm) of the calf muscle were prepared at levels 50

μm apart from each other and used for hematoxylin and eosin (HE) staining to localize the transplant. Levels containing the transplant were stained immunohistochemically for the presence of insulin, as described previously,²¹ and glucagon. The primary antibody against glucagon (#2760, Cell Signaling, Danvers, MA, USA) was diluted in PBS containing 1% BSA (1:500). Antigen retrieval was performed in 10 mM sodium citrate buffer, pH 6.0, for 10 min at 99 °C. Subsequently, sections were incubated for 10 min with 3% H₂O₂ in PBS at room temperature in the dark, to block endogenous peroxidase activity. Nonspecific binding was blocked by incubation for 30 min with 5% goat serum. Primary antibody incubation for 60 min was followed by incubation with the secondary goat-rabbit biotin (1:200) (BA-1000, Vector Laboratories, Burlingame, CA, USA) and subsequently with the ABC complex (Vectastain, ABC kit, Elite). Finally, Bright DAB (BS04500, Immunologic BV, Duiven, Netherlands) was used for visualization.

RESULTS

Radiolabeling. After purification, [¹²⁵I]IBZM with a specific activity of 81.4 GBq/μmol was obtained with a radiochemical purity exceeding 99% as determined by RP-HPLC. Iodination using 1.2 mg/mL chloramine-T hydrate resulted in moderate regioselectivity: (1) 7.8% [¹²⁵I]-5-IBZM, (2) 59.7% [¹²⁵I]-3-IBZM, and (3) 32.5% [¹²⁵I]-3,5-di-IBZM, respectively. The second peak of the elution profile was identified as [¹²⁵I]-3-IBZM because it showed equal HPLC retention time as [¹²³I]-3-IBZM. Increasing amounts of the oxidant resulted in higher yields of the di-iodo analogue, [¹²⁵I]-3,5-di-IBZM. The binding properties of the different fractions to INS-1 cells are shown in Figure 2. After 4 h, 9.51 ± 1.13 fmol of [¹²⁵I]-3-IBZM was bound to the INS-1 cells, whereas only 0.69 ± 0.07 fmol of [¹²⁵I]-5-IBZM and 1.20 ± 0.14 fmol of the di-iodo analogue [¹²⁵I]-3,5-di-IBZM was bound to the INS-1 cells. These results show that [¹²⁵I]-3-IBZM had optimal D2 receptor binding properties. To increase regioselectivity for [¹²⁵I]-3-IBZM, the concentration of chloramine-T hydrate was lowered to 0.9 and 0.6 mg/mL. The iodination using 0.6 mg/mL chloramine-T hydrate, shown in Figure 2, resulted in 86.4% [¹²⁵I]-3-IBZM, 9.9% [¹²⁵I]-5-IBZM, and 3.7% [¹²⁵I]-3,5-di-IBZM. Iodination using 0.9 mg/mL chloramine-T resulted in only 77% [¹²⁵I]-3-IBZM.

Internalization Kinetics. Figure 3 summarizes the internalization kinetics of [¹²⁵I]-3-IBZM by INS-1 cells as determined

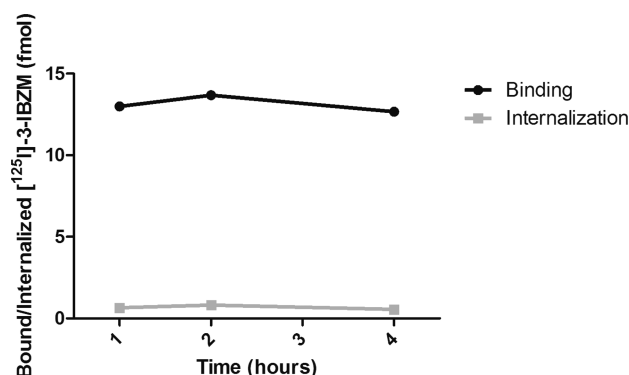


Figure 3. In vitro internalization kinetics of [^{125}I]-3-IBZM. The black line represents the surface bound fraction of [^{125}I]-3-IBZM. The gray line represents the internalized fraction of [^{125}I]-3-IBZM.

in vitro. As expected for an antagonist, there was no or very little internalization (0.65 ± 0.03 fmol, 3.2%) observed after 1 h. At this time point, 13.0 ± 0.7 fmol (63.4%) was bound to the D2 receptor. After 2 and 4 h respectively, no significant differences in binding or internalization were observed.

Pancreatic Islet Isolation and Transplantation. After the islet isolation procedure, islet viability and islet purity exceeded 90%. During overnight recovery in complete RPMI medium, islets regained their original morphology, as determined microscopically. Transplantation did not cause unexpected events in the recipient rats.

Binding Capacity of [^{125}I]IBZM to Isolated Islets.

Figure 4 shows the in vitro binding characteristics of [^{125}I]-3-

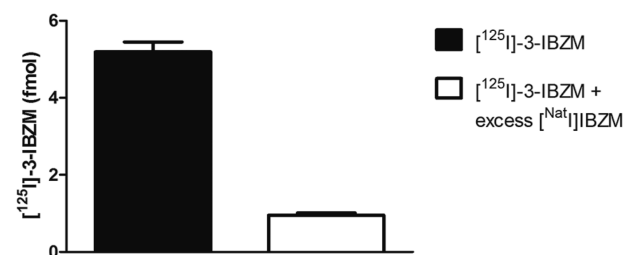


Figure 4. Binding capacity of [^{125}I]-3-IBZM to isolated islets. The solid bar represents the binding of [^{125}I]-3-IBZM. The white bar represents the binding of [^{125}I]-3-IBZM in the presence of an excess of [^{125}I]IBZM.

IBZM to 600 isolated islets of WAG/Rij rats. After 4 h, 5.19 ± 0.51 fmol [^{125}I]-3-IBZM was bound to the islets. Addition of 10 μg of unlabeled IBZM reduced the binding to 0.95 ± 0.12 fmol, indicating specific binding of the tracer to the D2 receptor on the islets of Langerhans.

SPECT/CT Imaging. The transplanted islets of Langerhans in the hind leg were visualized by SPECT, 1 h after injection of [^{123}I]IBZM. Six weeks after transplantation, a clear SPECT signal of [^{123}I]IBZM was observed in the transplanted islets in the calf muscle (Figure 5).

Biodistribution Study. Figure 6 summarizes the results of the biodistribution study. Biodistribution in WAG/Rij rats 2 h post injection showed tracer uptake in various organs such as the lung, spleen, liver, kidney, and duodenum. The relatively high uptake in the stomach ($4.43 \pm 0.57\%$ ID/g) was caused by the presence of free iodine after hepatic breakdown of the tracer. Due to the small volume of the transplant, as compared to the volume of the calf muscle, no significant difference in

tracer uptake was observed between the muscle containing the transplant and the control muscle.

Immunohistochemistry. All transplants could be localized within the muscle using HE staining. The transplants' location determined by HE staining colocalized with insulin staining and glucagon staining of consecutive sections, as shown in Figure 7. Furthermore, all transplants ($n = 3$) showed clear insulin and glucagon staining, indicating viable, insulin and glucagon producing beta and alpha cells in the transplant.

DISCUSSION

Ever since the presence of D2 receptors on rodent and human islets was revealed, it was pointed out as a possible target for beta cell imaging.²² Accordingly, IBZM imaging of transplanted islets has been proposed but the true potential of this tracer for beta cell imaging remained to be elucidated. Here, we have clearly demonstrated the possibility to visualize transplanted islets in vivo by specific targeting of the D2 receptor with [^{123}I]IBZM in a rat model.

In the 1980s, a variety of benzamide derivatives, all harboring strong antidopaminergic effects and high specificity for the D2 receptor, were discovered.²³ In 1988 Kung et al. described the synthesis of [^{125}I]IBZM and its application for D2 receptor mapping in the CNS.¹⁵ In the labeling procedure, some “minor impurities” were mentioned. Here, for the first time, we identified these “impurities” as the para-isomer and the di-iodo analogue. Furthermore, we determined the D2 receptor binding capacity of each labeled analogue in vitro and optimized the labeling to produce predominantly the ortho-isomer, [^{125}I]-3-IBZM. At optimized conditions, carrier free [^{125}I]-3-IBZM was synthesized at a specific activity of 81.4 GBq/ μmol with a radiochemical purity exceeding 99% after HPLC purification. The high specificity for the D2 receptor and the straightforward labeling procedure with high yields make IBZM an excellent tracer for islet graft imaging.

After the discovery of D2 receptors on beta cells of pancreatic islets in 2005,¹⁷ D2 receptor ligands were being applied to image pancreatic islets. ^{18}F -L-3,4-Dihydroxyphenylalanine positron emission tomography (^{18}F -DOPA PET) scans can be used to image congenital hyperinsulinism of infancy (CHI)^{24,25} and neuroendocrine tumors (NETs) such as insulinomas.²⁶ Due to their neuroendocrine nature, islets hold the ability to decarboxylate L-DOPA and accumulate the tracer according to the amine precursor uptake and decarboxylation (APUD) concept of Pearse.²⁷ However, although the total pancreatic uptake of [^{123}I]IBZM is similar to the uptake of exendin, the significant background signal from the exocrine tissue precludes quantitative imaging of native islets in the pancreas by D2 receptor targeting. Another potential issue might be the expression of D2 receptors on delta cells.²⁸ However, since delta cells only represent five percent of islet cells, it is very unlikely that tracer binding to the delta cells would significantly influence viable graft volume measurements by D2 receptor targeting.

Although islet imaging in the native pancreas is not feasible by targeting the D2 receptor due to the diffuse D2 receptor expression in this organ, it might be valuable in the transplantation setting. In 2011, Garcia et al. showed that islets, transplanted in the spleen, could be visualized using ^{18}F -fallypride PET.²⁹ Furthermore, transplanted islets could be visualized using ^{18}F -DOPA PET.³⁰ In this study, however, we preferred [^{123}I]IBZM in view of the favorable spatial resolution of preclinical SPECT systems as compared to PET.³¹

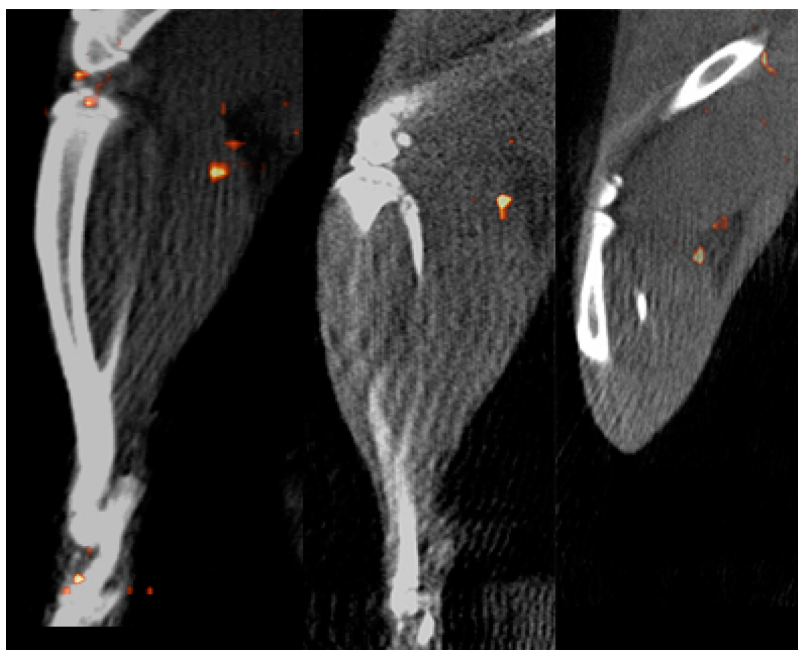


Figure 5. In vivo SPECT/CT images of the islets engrafted in the muscle of rats ($n = 3$), 6 weeks after transplantation, acquired 1 h after injection of $[^{123}\text{I}]\text{IBZM}$.

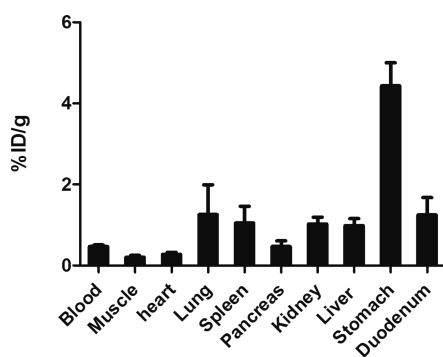


Figure 6. Biodistribution of $[^{123}\text{I}]\text{IBZM}$ in WAG/Rij rats ($n = 3$). Values are expressed as percentages injected dose per gram tissue. Rats were dissected 2 h post injection.

Furthermore, the spleen, kidney, and liver, wherein islets are most often transplanted both preclinically and clinically, show considerable $[^{123}\text{I}]\text{IBZM}$ uptake (Figure 6), precluding islet graft detection using IBZM in these organs. Therefore, striated

muscle appeared to be an excellent transplantation site to determine the value of D2 receptor targeting for islet imaging. In this model, islet grafts could clearly be delineated as areas of focal uptake, when compared to PET imaging of islets engrafted in the spleen or subcutaneously,^{29,30} representing substantial progress in molecular imaging of islet grafts.

Both for D2 receptor targeting and for graft survival, striated muscle harbors advantages as a transplantation site when compared to liver and the kidney capsule. A common problem in both liver and kidney capsule transplantation is insufficient revascularization resulting in impaired islet oxygenation.^{32,33} However, it has been shown that islets transplanted in the muscle show high vascular density and oxygenation.³⁴ It was even stated that islets engrafted in the muscle create a vascular system which resembles the native pancreas³⁵ and patients were transplanted successfully in the muscle.³⁶ Since the muscle is considered a promising novel site for islet transplantation, islet graft imaging via D2 receptor targeting might contribute to the further improvement of this promising therapy, despite its limited imaging capacities for liver grafts.

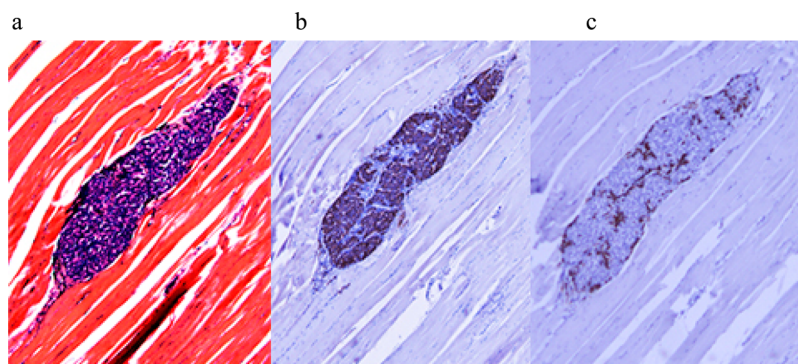


Figure 7. HE staining (A) (100 \times), insulin staining (B) (100 \times), and glucagon staining (C) (100 \times) of three consecutive slices of muscle tissue containing the transplant.

In view of the D2 receptor mediated binding to isolated islets in vitro and the distinct tracer uptake in the SPECT images, the present study clearly demonstrates that [^{123}I]IBZM can be used to monitor the viability of islet grafts following transplantation in future studies. Nevertheless, in combination with other beta cell specific radiotracers such as ^{111}In -exendin, it might provide complementary information on the metabolic state of the islet graft. To summarize, IBZM imaging could provide vital complementary information on the viability and functionality of the islet graft. This may lead to early detection of aberrant processes in the transplant and eventually might improve the success of islet transplantation.

CONCLUSION

The labeling procedure was optimized to produce predominantly [^{125}I]-3-IBZM at a high specific activity and radiochemical purity. The tracer showed D2 receptor-mediated binding to isolated islets and uptake within the transplant. Engrafted islets were clearly visualized on SPECT/CT images after injection of [^{123}I]BZM. In conclusion, [$^{123/125}\text{I}$]BZM is a suitable tracer for islet graft imaging in vivo, and its imaging capacities for transplanted islets will be further elucidated.

AUTHOR INFORMATION

Corresponding Author

*Tel/fax: +31 24 36 19097/+31 24 36 18942. E-mail: Stefanie.willekens@radboudumc.nl.

Notes

The authors declare no competing financial interest.

ACKNOWLEDGMENTS

We thank Bianca Lemmers, Henk Arnts, Iris Lamers, and Kitty Lemmers for their technical support with the animal experiments. The research leading to these results has received funding from the People Programme (Marie Curie Actions) of the European Union's Seventh Framework Programme FP7/2007-2013/ under REA grant agreement No. 289932.

REFERENCES

- (1) McCall, M.; Shapiro, A. M. J. Update on islet transplantation. *Cold Spring Harbor Perspect. Med.* **2012**, *2* (7), a007823.
- (2) Berney, T.; Toso, C. Monitoring of the islet graft. *Diabetes Metab.* **2006**, *32* (5 Part 2), S03–12.
- (3) Weir, G. C.; Bonner-Weir, S. Five stages of evolving beta-cell dysfunction during progression to diabetes. *Diabetes* **2004**, *53* (Suppl. 3), S16–21.
- (4) Ritzel, R. A.; Butler, A. E.; Rizza, R. A.; Veldhuis, J. D.; Butler, P. C. Relationship between beta-cell mass and fasting blood glucose concentration in humans. *Diabetes Care* **2006**, *29* (3), 717–8.
- (5) Gotthardt, M.; Eizirik, D. L.; Cnop, M.; Brom, M. Beta cell imaging - a key tool in optimized diabetes prevention and treatment. *Trends Endocrinol. Metab.* **2014**, *25* (8), 375–7.
- (6) Eriksson, O.; Alavi, A. Imaging the islet graft by positron emission tomography. *Eur. J. Nucl. Med. Mol. Imaging* **2012**, *39* (3), 533–42.
- (7) Jirak, D.; Kriz, J.; Herynek, V.; Andersson, B.; Girman, P.; Burian, M.; Saudek, F.; Hajek, M. MRI of transplanted pancreatic islets. *Magn. Reson. Med.* **2004**, *52* (6), 1228–33.
- (8) Evgenov, N. V.; Medarova, Z.; Dai, G.; Bonner-Weir, S.; Moore, A. In vivo imaging of islet transplantation. *Nat. Med.* **2006**, *12* (1), 144–8.
- (9) Lu, Y.; Dang, H.; Middleton, B.; Zhang, Z.; Washburn, L.; Stout, D. B.; Campbell-Thompson, M.; Atkinson, M. A.; Phelps, M.; Gambhir, S. S.; Tian, J.; Kaufman, D. L. Noninvasive imaging of islet grafts using positron-emission tomography. *Proc. Natl. Acad. Sci. U. S. A.* **2006**, *103* (30), 11294–9.
- (10) Kim, S. J.; Doudet, D. J.; Studenov, A. R.; Nian, C.; Ruth, T. J.; Gambhir, S. S.; McIntosh, C. H. Quantitative micro positron emission tomography (PET) imaging for the in vivo determination of pancreatic islet graft survival. *Nat. Med.* **2007**, *12* (12), 1423–8.
- (11) Toso, C.; Zaidi, H.; Morel, P.; Armanet, M.; Andres, A.; Pernin, N.; Baertschiger, R.; Slosman, D.; Buhler, L. H.; Bosco, D.; Berney, T. Positron-emission tomography imaging of early events after transplantation of islets of Langerhans. *Transplantation* **2005**, *79* (3), 353–5.
- (12) Kalliokoski, T.; Simell, O.; Haaparanta, M.; Viljanen, T.; Solin, O.; Knuuti, J.; Nuutila, P. An autoradiographic study of [^{18}F]FDG uptake to islets of Langerhans in NOD mouse. *Diabetes Res. Clin. Pract.* **2005**, *70* (3), 217–24.
- (13) Pattou, F.; Kerr-Conte, J.; Wild, D. GLP-1-receptor scanning for imaging of human beta cells transplanted in muscle. *N. Engl. J. Med.* **2010**, *363* (13), 1289–90.
- (14) de Geus-Oei, L. F.; Zerizer, I.; Uebleis, C.; Al-Nahas, A. Highlights of the EANM Congress 2011: Birmingham, UK. *Eur. J. Nucl. Med. Mol. Imaging* **2012**, *39* (2), 354–68.
- (15) Kung, H. F.; Kasliwal, R.; Pan, S. G.; Kung, M. P.; Mach, R. H.; Guo, Y. Z. Dopamine D-2 receptor imaging radiopharmaceuticals: synthesis, radiolabeling, and in vitro binding of (R)-(+)- and (S)-(–)-3-iodo-2-hydroxy-6-methoxy-N-[(1-ethyl-2-pyrrolidinyl)methyl]-benzamide. *J. Med. Chem.* **1988**, *31* (5), 1039–43.
- (16) de Paulis, T. The discovery of epidepride and its analogs as high-affinity radioligands for imaging extrastriatal dopamine D(2) receptors in human brain. *Curr. Pharm. Des.* **2003**, *9* (8), 673–96.
- (17) Rubi, B.; Ljubicic, S.; Pournourmohammadi, S.; Carobbio, S.; Armanet, M.; Bartley, C.; Maechler, P. Dopamine D2-like receptors are expressed in pancreatic beta cells and mediate inhibition of insulin secretion. *J. Biol. Chem.* **2005**, *280* (44), 36824–32.
- (18) Shankar, E.; Santhosh, K. T.; Paulose, C. S. Dopaminergic regulation of glucose-induced insulin secretion through dopamine D2 receptors in the pancreatic islets in vitro. *IUBMB Life* **2006**, *58* (3), 157–63.
- (19) Asfari, M.; Janjic, D.; Meda, P.; Li, G.; Halban, P. A.; Wollheim, C. B. Establishment of 2-mercaptoethanol-dependent differentiated insulin-secreting cell lines. *Endocrinology* **1992**, *130* (1), 167–78.
- (20) Laverman, P.; Roosenburg, S.; Gotthardt, M.; Park, J.; Oyen, W. J.; de Jong, M.; Hellmich, M. R.; Rutjes, F. P.; van Delft, F. L.; Boerman, O. C. Targeting of a CCK(2) receptor splice variant with (111)In-labelled cholecystokinin-8 (CCK8) and (111)In-labelled minigastrin. *Eur. J. Nucl. Med. Mol. Imaging* **2008**, *35* (2), 386–92.
- (21) Brom, M.; Woliner-van der Weg, W.; Joosten, L.; Frielink, C.; Bouckennooghe, T.; Rijken, P.; Andralojc, K.; Goke, B. J.; de Jong, M.; Eizirik, D. L.; Behe, M.; Lahoutte, T.; Oyen, W. J.; Tack, C. J.; Janssen, M.; Boerman, O. C.; Gotthardt, M. Non-invasive quantification of the beta cell mass by SPECT with ^{111}In -labelled exendin. *Diabetologia* **2014**, *57*, 950.
- (22) Brom, M.; Andralojc, K.; Oyen, W. J.; Boerman, O. C.; Gotthardt, M. Development of radiotracers for the determination of the beta-cell mass in vivo. *Curr. Pharm. Des.* **2010**, *16* (14), 1561–7.
- (23) de Paulis, T.; Kumar, Y.; Johansson, L.; Raemssby, S.; Florvall, L.; Hall, H.; Aengeby-Moeller, K.; Oegren, S. O. Potential neuroleptic agents. 3. Chemistry and antidopaminergic properties of substituted 6-methoxysalicylamides. *J. Med. Chem.* **1985**, *28* (9), 1263–9.
- (24) Otonkoski, T.; Nanto-Salonen, K.; Seppanen, M.; Veijola, R.; Huopio, H.; Hussain, K.; Tapanainen, P.; Eskola, O.; Parkkola, R.; Ekstrom, K.; Guiot, Y.; Rahier, J.; Laakso, M.; Rintala, R.; Nuutila, P.; Minn, H. Noninvasive diagnosis of focal hyperinsulinism of infancy with [^{18}F]-DOPA positron emission tomography. *Diabetes* **2006**, *55* (1), 13–8.
- (25) Mohnike, K.; Blankenstein, O.; Minn, H.; Mohnike, W.; Fuchtnner, F.; Otonkoski, T. [^{18}F]-DOPA positron emission tomography for preoperative localization in congenital hyperinsulinism. *Horm. Res.* **2008**, *70* (2), 65–72.

- (26) Becherer, A.; Szabo, M.; Karanikas, G.; Wunderbaldinger, P.; Angelberger, P.; Raderer, M.; Kurtaran, A.; Dudczak, R.; Kletter, K. Imaging of advanced neuroendocrine tumors with (18)F-FDOPA PET. *J. Nucl. Med.* **2004**, *45* (7), 1161–7.
- (27) Pearse, A. G. The cytochemistry and ultrastructure of polypeptide hormone-producing cells of the APUD series and the embryologic, physiologic and pathologic implications of the concept. *J. Histochem. Cytochem.* **1969**, *17* (5), 303–13.
- (28) Chen, Y.; Hong, F.; Chen, H.; Fan, R. F.; Zhang, X. L.; Zhang, Y.; Zhu, J. X. Distinctive expression and cellular distribution of dopamine receptors in the pancreatic islets of rats. *Cell Tissue Res.* **2014**, *357* (3), 597–606.
- (29) Garcia, A.; Mirbolooki, M. R.; Constantinescu, C.; Pan, M. L.; Sevioukov, E.; Milne, N.; Wang, P. H.; Lakey, J.; Chandy, K. G.; Mukherjee, J. 18F-Fallypride PET of pancreatic islets: in vitro and in vivo rodent studies. *J. Nucl. Med.* **2011**, *52* (7), 1125–32.
- (30) Eriksson, O.; Mintz, A.; Liu, C.; Yu, M.; Naji, A.; Alavi, A. On the use of [18F]DOPA as an imaging biomarker for transplanted islet mass. *Ann. Nucl. Med.* **2014**, *28* (1), 47–52.
- (31) Deleye, S.; Van Hoken, R.; Verhaeghe, J.; Vandenberghe, S.; Stroobants, S.; Staelens, S. Performance evaluation of small-animal multipinhole muSPECT scanners for mouse imaging. *Eur. J. Nucl. Med. Mol. Imaging* **2013**, *40* (5), 744–58.
- (32) Lau, J.; Carlsson, P. O. Low revascularization of human islets when experimentally transplanted into the liver. *Transplantation* **2009**, *87* (3), 322–5.
- (33) Mattsson, G.; Jansson, L.; Carlsson, P. O. Decreased vascular density in mouse pancreatic islets after transplantation. *Diabetes* **2002**, *51* (5), 1362–6.
- (34) Svensson, J.; Lau, J.; Sandberg, M.; Carlsson, P. O. High vascular density and oxygenation of pancreatic islets transplanted in clusters into striated muscle. *Cell transplantation* **2011**, *20* (5), 783–8.
- (35) Christoffersson, G.; Henriksnas, J.; Johansson, L.; Rolny, C.; Ahlstrom, H.; Caballero-Corbalan, J.; Segersvard, R.; Permert, J.; Korsgren, O.; Carlsson, P. O.; Phillipson, M. Clinical and experimental pancreatic islet transplantation to striated muscle: establishment of a vascular system similar to that in native islets. *Diabetes* **2010**, *59* (10), 2569–78.
- (36) Rafael, E.; Tibell, A.; Ryden, M.; Lundgren, T.; Savendahl, L.; Borgstrom, B.; Arnelo, U.; Isaksson, B.; Nilsson, B.; Korsgren, O.; Permert, J. Intramuscular autotransplantation of pancreatic islets in a 7-year-old child: a 2-year follow-up. *Am. J. Transplant.* **2008**, *8* (2), 458–62.